

PAPER • OPEN ACCESS

Mineralogical Study on the Consistency Property of Bentonite Mixed Soil

To cite this article: M Okawara *et al* 2021 *IOP Conf. Ser.: Earth Environ. Sci.* **849** 012005

View the [article online](#) for updates and enhancements.

You may also like

- [Revealing Hexadecyltrimethylammonium Chloride \(HDTA\) Intercalated Bentonite in Sulfonated Poly\(ether ether ketone\) as Nanocomposite Membrane Electrolyte for Direct Methanol Fuel Cells](#)
S. Sasikala, Gutru Rambabu, Avanish Shukla et al.
- [Active adsorption performance of planetary ball milled Saudi Arabian bentonite clay for the removal of copper ions from aqueous solution](#)
Ahmed Abutaleb, Mubarak A. Eldoma, Mohd Imran et al.
- [Purification and activation of the Iraqi bentonite for edible oil Production](#)
Hameed R D Alameery and Saad A Ahmed



ECS Membership = Connection

ECS membership connects you to the electrochemical community:

- Facilitate your research and discovery through ECS meetings which convene scientists from around the world;
- Access professional support through your lifetime career;
- Open up mentorship opportunities across the stages of your career;
- Build relationships that nurture partnership, teamwork—and success!

Join ECS!

Visit electrochem.org/join



Mineralogical Study on the Consistency Property of Bentonite Mixed Soil

M Okawara^{1*}, Y Saito², K Ishiguro² and Y Hotta²

¹Iwate University, Faculty of Science and Engineering, 4-3-5 Ueda, Morioka City, Iwate Prefecture, Japan

²Graduate School of Engineering, Iwate University, 4-3-5 Ueda, Morioka, Iwate, Japan

E-mail: okawara@iwate-u.ac.jp

Abstract. Bentonite mixed soil, which is a mixture of bentonite with sand and gravel, can be easily compacted by adjusting the blending degree, and it is difficult for water to pass through and exhibits low permeability. It is widely used at construction sites because it can be mixed on-site and has good workability. Examples of its use include impermeable layers at waste disposal sites and measures to contain heavy metals from rocks generated from construction sites. The main component of bentonite is smectite, which is a swelling clay mineral, and the swelling property and consistency characteristics determine the engineering properties. In particular, low permeability is considered to be strongly influenced by the electrochemical properties at the crystal level peculiar to smectite. In this study, the mechanism of expression of engineering properties of bentonite mixed soil was investigated focusing on the mineralogy properties of smectite. Specifically, X-ray and near-infrared analysis were performed to clarify the crystal structure of smectite and the adsorptivity of water molecules. The change in interlayer distance were clarified by XRD. Information on the behavior of water molecules was obtained by NIR. From these analyses, we obtained information on the swelling, consistency and micro-physical properties of smectite, which is the main component of bentonite, related to water permeability.

1. Introduction

The use of bentonite, which is primarily composed of smectite, as a cushioning material for the geological disposal of high-level radioactive waste is being researched in various countries; Finland has already begun construction on disposal sites set to start operating in FY 2020. Bentonite is being used as a cushioning material because its primary component, smectite, is expected to offer water cut-off, self-sealing properties, delayed sorption or migration of nuclides, and chemical buffering properties [1]. To construct and operate sites, and ensure that these properties are expressed effectively, the fundamental properties of smectite first need to be experimentally verified.

One fundamental property of smectite is swelling. Smectite, which is a type of layered silicate mineral, increases its volume by the intake of water molecules between its layers. The swelling processes that occur in smectite can be broadly divided into two types: crystalline swelling in low-water-content areas and osmotic swelling in high-water-content areas [2]. Given that the construction of a geological disposal facility requires conditions of relatively high dry density, it is important to clarify the properties expressed in the crystalline swelling process.

There is a long history of research into the state of smectite-water systems in the crystalline swelling process, and that work has produced many findings [3-8]. For instance, when the spacing of smectite is measured under controlled humidity, it yields discontinuous values such as 1 nm, 1.2-1.3 nm, 1.5-1.6



nm, and 1.8-1.9 nm. These values correspond to smectite when it has no interlayer water molecules (0WL), one interlayer water molecule (1WL), two interlayer water molecules (2WL), and three interlayer water molecules (3WL), respectively. Furthermore, it is a known fact that the humidity dependence of d-spacing varies widely depending on the type of exchangeable cation.

In addition, experiments [9, 10] and computer simulations [11, 12] have demonstrated that the motion of water molecules within layers is more controlled than bulk substances. Research on the motion of water molecules has been based on results from research on the crystal structure mentioned above. However, consistent conclusions have not been obtained due to differences in samples and experimental conditions, and researchers cannot claim to have a comprehensive picture of the properties of smectite-water systems.

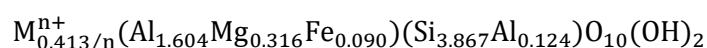
This study used X-ray diffraction and near-infrared spectroscopy to measure the crystal structure of high-purity homo-ionic smectite and the vibratory motion of water molecules under controlled humidity. To compare the experimental results in detail, measurements were taken at intervals of 5% relative humidity (RH) between 0 and 100% RH on adsorption and desorption processes.

2. Materials and methods

2.1. Materials and purification

We used Kunipia-F (Kunimine Industries Co., Ltd.), whose primary component is sodium smectite. Kunipia-F is an elutriated bentonite produced in Tsukinuno, Yamagata Prefecture that has an extremely high smectite content, 98 wt% [13]. However, some studies report that exchangeable cations contain about 20% Ca²⁺ and the like, in addition to Na⁺ [14].

In this study, we refined Kunipia-F to produce high-purity homo-ionic (Na⁺, K⁺, Mg²⁺, Ca²⁺) smectite. Refining was a two-step process involving centrifugal separation to remove accessory minerals and ion exchange to make homo-ionic exchangeable cations. The prepared samples underwent X-ray diffraction analysis, exchangeable cation analysis, and removal of accessory minerals and homo-ionization was confirmed. The structural formula for the refined smectite from Tsukinuno is shown below [14].



2.2. Water content adjustment

Water molecule adsorption was studied under controlled humidity to adjust water content. The humidity control unit is composed of a saturation chamber, temperature, pressure, and flow rate controller, in addition an experimental chamber. The water vapor content of the saturation chamber is controlled using temperature and pressure settings, and moist air is sent into the experimental chamber, as the flow rate is adjusted to produce the desired humidity level. The temperature of the experimental chamber was set to room temperature (25°C).

2.3. X-ray diffraction

After oven-drying the powdered sample at 200°C for 24 hours, the sample was cooled at room temperature inside a desiccator and filled into the sample holder of an air separator (Rigaku). After placing the sample in the experimental chamber (with the humidity adjusted) and waiting for water molecule adsorption to reach equilibrium, the sample holder was made airtight with a sample case, an X-ray diffraction device was attached, and measurements were taken. Equilibrium is deemed to have been reached when the shape of the X-ray diffraction profile does not undergo significant changes.

The Ultima IV horizontal multipurpose sample X-ray diffractometer (manufactured by Rigaku) was used to take measurements. The measurement conditions were as follows: X-ray diffractometer with CuK α radiation using 40kV, 40mA, measurement method: FT measurement, step width: 0.0600°, gate time: 1 s, scanned from 2° to 50° 2 θ .

2.4. Near-infrared spectroscopy

After oven-drying the powdered sample at 200°C for 24 hours, the sample was cooled at room temperature inside a desiccator and filled into a glass container. After placing the sample in the experimental chamber (with the humidity adjusted) and waiting for water molecule adsorption to reach equilibrium, measurements were taken. Equilibrium is deemed to have been reached when the shape of the near-infrared absorption spectrum no longer undergoes significant changes.

The Spectrum 400 Fourier transform infrared spectrometer (manufactured by Perkin Elmer) was used for measurements. The measurement conditions were as follows: Measurement method: diffuse reflection, resolving power: 4 cm⁻¹, number of additions: 100 times, measurement range: 4000-7800 cm⁻¹.

3. Crystal structure of smectite

Figure 1 shows an example of an X-ray diffraction profile. The peak at the top of the profile is due to Bragg reflection, and the following relationship exists between crystal d-spacing and diffraction angle 2θ.

$$n\lambda = 2d \sin \theta \quad (1)$$

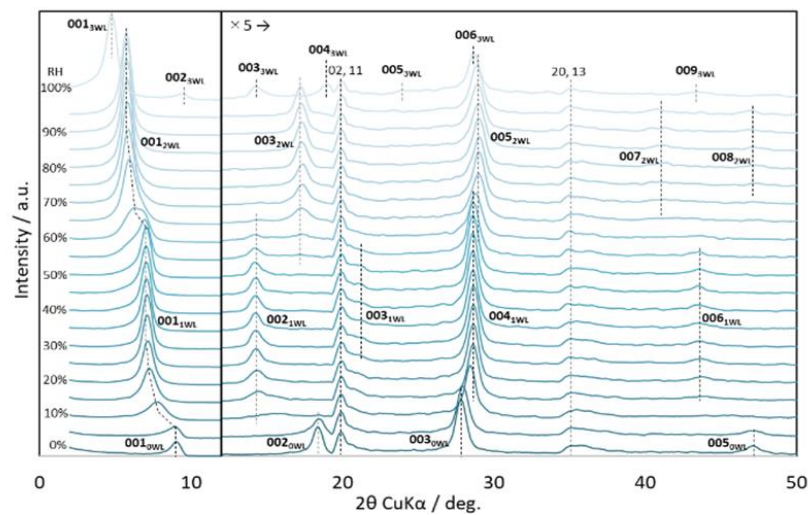


Figure 1. XRD profiles of Na-smectite on desorption process.

Here, n is a positive integer and λ is the wavelength of the X-ray. d_{001} spacing is found by substituting the diffraction angle of reflection 001 observed in $2\theta < 10^\circ$ into Formula (1). Meanwhile, reflection 00ℓ observed in $2\theta < 10^\circ$ corresponds to the n th reflection of reflection 001. The position of 00ℓ reflection changes discontinuously according to the state of water content.

3.1. Interstratification

A multiple water-content states coexist is referred to as interstratification. For instance, when RH is 60% at the point where 2WL changes to 1WL in Figure 1, 002_{1WL} and 003_{2WL} coexist in the range of 10° to 20° . To ascertain specific information about crystal structure, the degree of interstratification must be evaluated.

Ferrage et al. (2005) [6] used the standard deviation to classify the regularity of 00ℓ reflection and evaluated the degree of interstratification ξ for smectite.

$$\xi = \sqrt{\frac{1}{X_i} \sum (x - \bar{x})^2} \quad (2)$$

$$x = \ell \times d_{00\ell} \quad (3)$$

Here, X_i is the number of 00ℓ reflections that can be measured by $2\theta = 2-50^\circ$. \bar{x} is the mean value of $\ell \times d_{00\ell}$. Ferrage et al. (2005) states that an interstratification state occurs when $\xi > 0.04$ nm, and the present study followed that definition as well.

3.2. Basal spacing

Figure 2 shows the humidity dependence of d_{001} spacing. Here, the darkness of the plot color represents the degree of interstratification ξ ; the lighter the color, the more marked the interstratification. Hysteresis was observed in all samples, and interstratification tended to occur in the change region of the water-content state. Previous researches [3, 4, 6-8, 15, 16] are also consistent with this, and we were able to obtain more detailed data.

Sodium smectite changed stepwise in the pattern 0WL-1WL-2WL-3WL while potassium smectite changed stepwise in the pattern 0WL-1WL. Potassium smectite entered a state of 1WL and 2WL interstratification at 100% RH. Furthermore, $\xi > 0.01$ nm in nearly all areas of 1WL potassium smectite, demonstrating that the effects of 0WL interstratification were continuous. Tamura et al. (2000) [5] and Ferrage et al. (2005) [6] have reported the same.

Magnesium and calcium smectite change in the pattern 0WL-2WL-3WL during the adsorption process and in the pattern 3WL-2WL-1WL during the desorption process. When magnesium smectite is in a 2WL state during the desorption process, spacing decreased continuously from 1.61 nm to 1.35 nm. As 1.35 nm is too small for 2WL, we will refer to the 1.35-1.40 nm range as 2WL' here. Additionally, when RH is near 0-50% during the adsorption process in magnesium smectite, rehydration behavior is found to be extremely slow. Kawano and Tomita (1989) [17] state that condensation slows down in dehydrated magnesium smectite because Mg^{2+} sinks into the six-membered rings of the surface of the silicate layer.

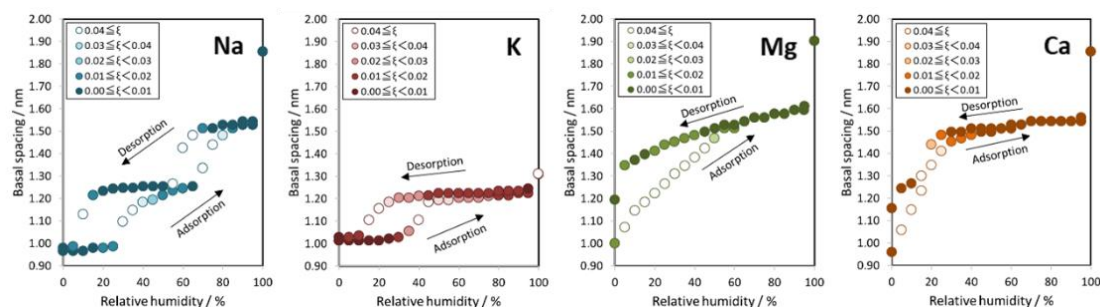


Figure 2. Changes in basal spacing d_{001} of Na-, K-, Mg- and Ca-smectite. The color of the circles indicates degree of interstratification.

4. Water molecules in smectite

Figure 3 shows an example of a near-infrared absorption spectrum. The absorption observed in this region is the combination tone ($\nu+\delta$) of the stretching vibration ν and angular vibration δ of OH groups. Absorption near $4300-4600\text{ cm}^{-1}$ is due to clay mineral OH groups and represented by $(\nu+\delta)_{\text{clay}}$, while absorption near $4700-5400\text{ cm}^{-1}$ is due to water molecule OH groups and represented by $(\nu+\delta)_{\text{water}}$. Furthermore, within the designation $(\nu+\delta)_{\text{water}}$, sharp components near 5250 cm^{-1} are attributed to OH groups that act upon the oxygen atoms of the silicate layer surface, while broad components near 5100 cm^{-1} are attributed to OH groups that act upon other water molecules [18]. The increase in the absorption area of $(\nu+\delta)_{\text{water}}$ represents an increase in water content [19].

4.1. Water content

We investigated the relationship between water content and the absorption area A_w of $(\nu+\delta)_{\text{water}}$ (Figure 4) obtained from the measurements shown in Figure 3. However, the absorption area A_w' on the horizontal axis was obtained by dividing A_w by A_c for standardization. As we found an extremely strong

correlation between water content and the absorption area A_w' in all samples, it used as a calibration curve to derive water content from the measured spectrum.

Figure 5 shows the humidity dependence of water content. Water content reflects changes in d-spacing. Previous researches [15, 16, 20, 21] are also consistent with this. Figure 6 shows the relationship between basal spacing and water content. Monovalent and divalent ions exhibit very different patterns. Specifically, changes in d-spacing relative to water content are discontinuous for monovalent ions and continuous for divalent ions. The continuous pattern is particularly strong in magnesium smectite. In the first place, discontinuous spacing values have long been attributed to the diameter of interlayer water molecules. There is a strong possibility that these continuous changes are due to divalent cations changing the arrangement of interlayer water. Furthermore, it has been demonstrated that water content is about $10\pm 5\%$ for 1WL, $20\pm 5\%$ for 2WL, and 30% for 3WL, regardless of the type of exchangeable cation.

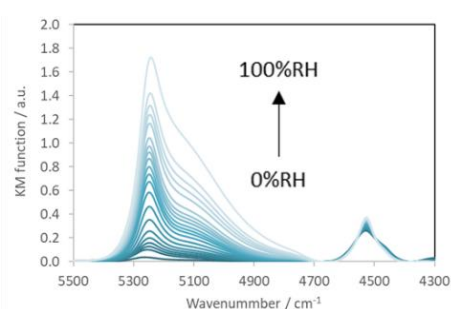


Figure 3. NIR spectra of Na-smectite on adsorption process.

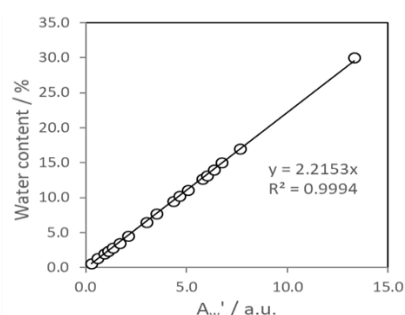


Figure 4. Relation between water content and normalized area of $(\nu+\delta)_{\text{water}} A_w'$ (Na-smectite) .

4.2. State of water molecules

Figure 7 shows different spectrum analysis results from $(\nu+\delta)_{\text{water}}$ organized by water content state. 2WL is divided into two sections because the characteristics of the spectrum shape are different on the low-humidity side and the high-humidity side. It is clear that different components change based on the water content state.

In the case of 1WL, change primarily occurs in the 5250 cm^{-1} component, while there is little change in the 5100 cm^{-1} component. Meanwhile, on the low-humidity side of 2WL, the 5100 cm^{-1} component changes more. It is clear that, from the high-humidity side of 2WL to 3WL, the spectrum shape approaches that of pure water.

Due to this, for 1WL, it is thought that both OH groups of each interlayer water molecule interact with the silicate layer surface facing them, and on the low-humidity side of 2WL, one OH group interacts with the silicate layer surface while the other OH group interacts with different water molecules. Furthermore, although components that are close to pure water in terms of vibratory motion increase from the high-humidity side of 2WL to 3WL, this is attributed to water molecules that exist between the two water molecule layers that act on the silicate layer. These results are consistent with those obtained in computer simulations [11, 22]. As describe above, it is clear that the vibratory motion of water molecules is highly dependent on water content state rather than the type of exchangeable cation.

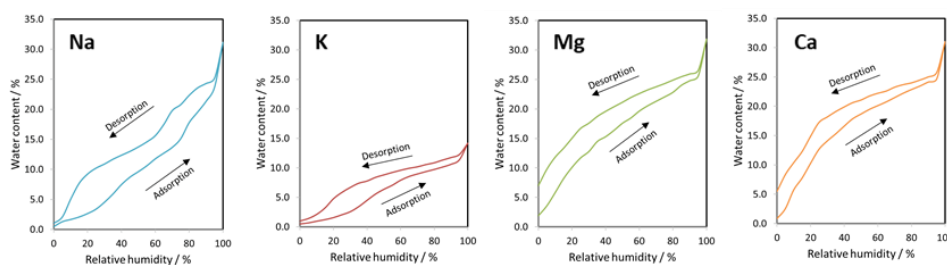


Figure 5. Changes in water content of Na-, K-, Mg- and Ca-smectite.

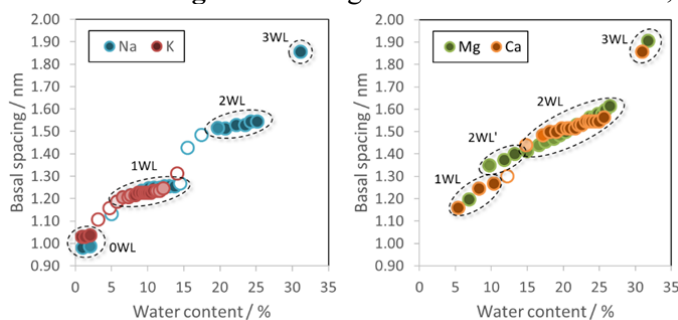


Figure 6. Relation between basal spacing and water content of Na-, K-, Mg- and Ca-smectite on desorption process.

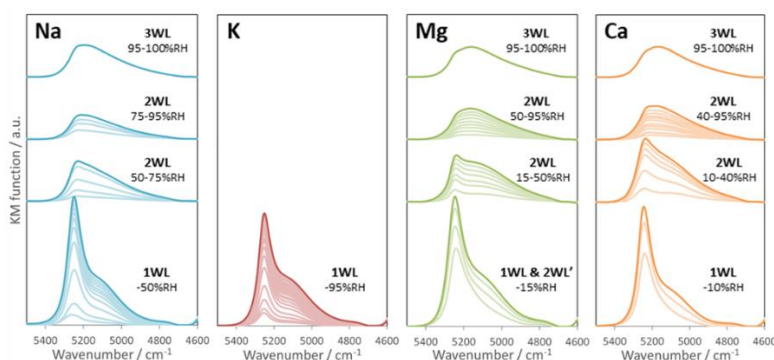


Figure 7. Different spectrums of Na-, K-, Mg- and Ca-smectite on desorption process.

EXAFS (Extended X-ray Absorption Fine Structure) analysis can provide informations on radial distances and coordination numbers around the specific elements. Figure 8 shows radial distances of Ca-smectite. We recognized that the distances from Ca^{2+} were different between water content of 80% and 200%.

4.3. Hydrolysis in Mg-smectite

$(\nu+\delta)_{\text{water}}$ in magnesium smectite exhibits a distinctive form in 0WL, namely, when RH is 0% during the adsorption process. In this state, water content is 1.9% and a simple calculation shows that there are two water molecules per Mg^{2+} . There is a strong possibility that Mg^{2+} with high ion potential changes the state of the surrounding water molecules. According to Maftuleac (2015) [23], the water molecules in smectite sometimes undergo hydrolysis due to polyvalent M^{n+} cations.



We hypothesized that H_3O^+ was produced by hydrolysis even in magnesium smectite, and we prepared hydrogen smectite and measured its spectrum. During this, the hydrogen smectite spectrum exhibited characteristics that were extremely similar to those of magnesium smectite (Figure 9). This leads us to conclude that, in magnesium smectite, hydrolysis produces H_3O^+ .

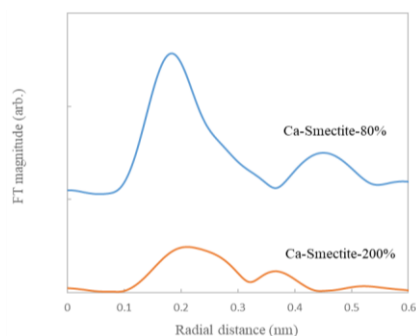


Figure 8. Radial distances of Ca-smectite.

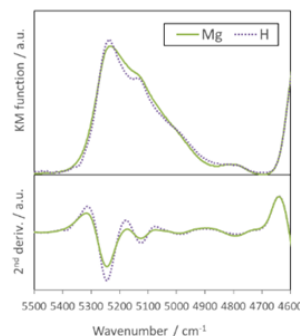


Figure 9. NIR and 2nd deviation spectrums of Mg- and H-smectite.

5. Conclusion

High-purity homo-ionic (Na^+ , K^+ , Mg^{2+} , Ca^{2+}) smectite was analyzed using X-ray diffraction and near-infrared spectroscopy, producing the below findings regarding crystal structure and the state of water molecules.

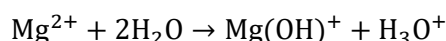
(1) Changes in d-spacing relative to water content are discontinuous for monovalent ions and continuous for divalent ions. There is a possibility that divalent ions with high ion potential change the arrangement of interlayer water molecules.

(2) For 1WL, both OH groups of interlayer water interact with the silicate layer surface facing them, and on the low-humidity side of 2WL, one OH group interacts with the silicate layer surface while the other OH group interacts with different water molecules.

(3) From the high-humidity side of 2WL to 3WL, there is also water that is similar to pure water in terms of vibratory motion.

(4) Water content is about $10 \pm 5\%$ for 1WL, $20 \pm 5\%$ for 2WL, and 30% for 3WL, regardless of the type of exchangeable cation.

(5) In magnesium smectite, hydrolysis produces H_3O^+ .



References

- [1] Sato H 2009 Function for controlling nuclide migration of buffer material in the geological disposal for high-level radioactive waste *MMIJ* **125** 1-12
- [2] Norrish K 1972 Forces between clay particles *Proc. 4th Int. Clay Conf.* 375-83
- [3] Iwasaki T 1979 Relationship between X-ray basal reflections and interlayer cations of montmorillonite: On the distribution of Ca and Na ions *J. Miner. Soc. Japan* **14** 78-89
- [4] Sato T, Watanabe T and Otsuka R 1992 Effects of layer charge, charge location, and energy change on expansion properties of dioctahedral smectites *Clays Clay Miner.* **40** 103-13
- [5] Tamura K, Yamada H and Nakazawa H 2000 Stepwise hydration of high-quality synthetic smectite with various cations *Clays Clay Miner.* **48** 400-4
- [6] Ferrage E, Lanson B, Sakharov B A and Drit V A 2005 Investigation of smectite hydration properties by modeling experimental X-ray diffraction patterns: Part I. Montmorillonite hydration properties *Am. Mineral.* **90** 1358-74
- [7] Morodome S and Kawamura K 2009 Swelling behavior of Na- and Ca-montmorillonite up to 150°C by in situ X-Ray diffraction experiments *Clays Clay Miner.* **57** 150-60
- [8] Morodome S and Kawamura K 2011 In situ X-ray diffraction study of the swelling of montmorillonite as affected by exchangeable cations and temperature *Clays Clay Miner.* **59** 165-75
- [9] Cebula D J, Thomas R K and White J W 1981 Diffusion of water in li-montmorillonite studied by quasielastic neutron scattering *Clays Clay Miner.* **29** 241-8

- [10] Gates W P, Aldridge L P, Carnero-Guzman G G, Mole R A, Yu D, Iles G N, Klapproth A and Bordallo H N 2017 Water desorption and absorption isotherms of sodium montmorillonite: A QENS study *Appl. Clay Sci.* **147** 97-104
- [11] Chang F R C, Skipper N T and Sposito G 1995 Computer simulation of interlayer molecular structure in sodium montmorillonite hydrates *Langmuir* **11** 2734-41
- [12] Yotsuji K, Tachi Y, Kawamura K, Arima T and Sakuma H 2019 Molecular dynamics simulations of physical properties of water and cations in montmorillonite interlayer: Application to diffusion model *Nendo Kagaku* **58** 8-25
- [13] Fujita T Study on sealing performance of clay plug for geological disposal of high-level radioactive waste, Doctoral thesis Saitama University
- [14] Suzuki K, Takagi S, Sato T and Yoneda T 2007 Preparation and characterization of highly purified montmorillonite *Nendo Kagaku* **46** 147-55
- [15] Bérend I, Cases J M, François M, Uriot J P, Michot L, Masion A and Thomas F 1995 Mechanism of adsorption and desorption of water vapor by homoionic montmorillonites: 2. The Li⁺ Na⁺, K⁺, Rb⁺ and Cs⁺-exchanged forms *Clays Clay Miner.* **43** 324-36
- [16] Cases J M, Bérend I, François M, Uriot J P, Michot L and Thomas F 1997 Mechanism of adsorption and desorption of water vapor by homoionic montmorillonite: 3. The Mg²⁺, Ca²⁺, Sr²⁺ and Ba²⁺ exchanged forms *Clays Clay Miner.* **45** 8-22
- [17] Kawano M and Tomita K 1989 X-RAY studies of rehydration behaviors for montmorillonite *Clay Sci.* **7** 277-87
- [18] Suzuki K, Kawamura K, Nakashima Y and Ichikawa Y 2003 The study of correlations between spectroscopic and dynamic properties of pore water in the clay-water system *Shigen to Sozai* **119** 581-6
- [19] Bizovská V, Pálková H and Madejová J 2016 Near-Infrared study of water adsorption on homoionic forms of montmorillonite *Clays Clay Miner.* **64** 571-85
- [20] Mooney R W, Keenan A G and Wood L A 1952 Adsorption of water vapor by montmorillonite. I. heat of desorption and application of BET theory *J. Am. Chem. Soc.* **74** 1367-71
- [21] Mooney R W, Keenan A G and Wood L A 1952 Adsorption of water vapor by montmorillonite. II. effect of exchangeable ions and lattice swelling as measured by X-Ray diffraction *J. Am. Chem. Soc.* **74** 1371-4
- [22] Suzuki S and Kawamura K 2004 Study of vibrational spectra of interlayer water in sodium beidellite by molecular dynamics simulations *J. Phys. Chem. B* **108** 13468-74
- [23] Maftuleac A 2015 The hydrated and hydrolyzed states of exchangeable cations in the montmorillonite and their quantitative assessment *International Journal of Materials Science and Applications* **4** 124-9